Check for updates

Article

JOURNAL OF COMPOSITE MATERIALS

Journal of Composite Materials
2018, Vol. 52(30) 4139–4150
© The Author(s) 2018
Article reuse guidelines:
sagepub.com/journals-permissions
DOI: 10.1177/0021998318776716
journals.sagepub.com/home/jcm
SAGE

Study of the ablative properties of phenolic/carbon composites modified with mesoporous silica particles

L Asaro[1], LB Manfredi[2] and ES Rodríguez[1]

Abstract

Mesoporous silica particles and carbon black were selected as fillers for a resol-type phenolic resin, to be used as a matrix for ablative materials. Composites were processed with the modified polymer and carbon fibers were used as continuous reinforcement. The ablative properties of the materials obtained were studied by the oxyacetylene torch test and the ablated samples were observed by scanning electron microscopy. Composites with 30 wt. % of carbon black achieved the lowest linear erosion rate and the highest insulation index, denoting the ability of the char produced to protect the virgin material. Considering that such composite has 44% by volume of carbon fibers, it could be inferred that its properties could be improved by increasing the fiber content and maintaining the amount of carbon black. The composite with 20 wt. % of mesoporous silica particles exhibited the lowest mass erosion rate, indicating a better stabilization of the char. Regarding dynamic-mechanical properties, the addition of particles induced a decrease in the modulus and glass transition temperature of all the systems studied.

Keywords

Ablation resistance, phenolic resin, carbon fibers, silica particles, composite materials

Introduction

In the aerospace industry, the materials used must meet requirements such as dimensional stability, high stiffness, and high temperature resistance. Thermal protection systems (TPS) are materials developed to protect structures from very aggressive atmospheres with high temperatures, high heat fluxes, and physical erosion.[1–3] These materials play an important role in the aerospace industry as they are used to shield aerodynamic structures, and in the construction of nozzle turbines and other components of rockets and aircraft engines. There are two main types of TPS: ablative and non-ablative ones. The former are materials that act through the loss of mass and are consumed during their use, whereas the latter use re-radiation of the incident heat as the main insulation mechanism. The typical formulations of ablative materials are based on polymer composites, although some are based on inorganic oxides and metals, whereas non-ablative materials are produced using ceramics or metals such as tungsten or rhenium.[4]

Phenolic resin/Carbon fiber-reinforced composites are appropriate as ablative TPS due to their high mechanical and thermal performance, and their ability to generate a protective carbonaceous residue.[5] Different thermosetting resins, such as epoxies, bismaleimides, and polyimides, have been used as matrices for ablative composites, but phenolics (in particular resol-type ones) are still the most used[4,6] due to their excellent flame and high-temperature resistance.[7] This resistance is partly attributed to the formation of a carbonaceous layer called "*char*", which radiates heat and acts as an insulating material, protecting the bulk material of the components.[8] When a layer of this *char* is consumed by the ablative process or is mechanically removed by the erosion of the combustion gases, another *char layer* is produced and the virgin material is protected. Regarding the reinforcements, they must

[1]Engineering Faculty, Structural Composite Materials, Research Institute of Material Science and Technology (INTEMA), National University of Mar del Plata, Argentina
[2]Engineering Faculty, Ecomaterials, Research Institute of Material Science and Technology (INTEMA), National University of Mar del Plata, Argentina

Corresponding author:
ES Rodríguez, J.B. Justo 4302, Mar del Plata 7600, Argentina.
Email: erodriguez@fi.mdp.edu.ar

provide the *char* with mechanical stability. Carbon fibers have been widely used as reinforcement in composites for thermal protection due to their high dimensional stability, non-flammability, low density, and excellent mechanical properties.[9] Composite materials based on phenolic resins and carbon fibers are used by NASA as standard material for high-temperature applications such as MX-4926.[10–14] This material also has micron-sized powdered fillers in the formulation, which are added to reduce the shrinkage of the resin and stabilize the charred polymer i.e. sensitive to the thermoerosion process that occurs in jet engines. Particles based on glass, refractory oxides, or carbon are typically used. However, traditional micron-sized ablation-resistant composites have shown a threshold in their protection capacity that cannot be surpassed unless a different approach is proposed. One of the limitations comes from the fact that *chars* are structurally weak and suffer mechanical erosion, reducing the lifetime of the ablative layer or requiring additional insulation thickness.[15,16] Materials with better ablative properties would permit applying relatively thinner protection layers, reducing the overall weight of aerospace systems. Thermoset polymer nanocomposites have excellent potential as ablative materials because, upon pyrolysis, the organic–inorganic nanostructure reinforcing the polymer can be converted into a uniform ceramic layer which may lead to significantly higher resistance to oxidation and mechanical erosion than traditional composite ablative materials.[17,18] Different nanoparticles such as nano-silica particles, carbon black (CB), carbon nanotubes, nanoclays, etc. have been used to enhance the ablation and thermal resistance of phenolic resins.[19–27] Srikanth et al. studied carbon/phenolic composites with nano-silica powder under the plasma arc jet and found that the nano-silica carbon/phenolic composites exhibited much higher ablation resistance than conventional carbon/phenolic composites under similar conditions. These authors attributed their results to a resistant silicon carbide phase produced by the added particles.[28] Ding et al. studied the effect of $ZrSi_2$ on the thermal degradation behavior of phenolic resin and the role of $ZrSi_2$ in the ablation resistance of carbon/phenolic composites, and found that the ablation resistance of carbon/phenolic composites was significantly improved by the incorporation of $ZrSi_2$ particles, with formation of ZrO_2 and SiO_2 during the oxygen/acetylene ablation process.[29] Park et al. studied the ablation properties and thermal conductivity of carbon nanotube and carbon fiber/phenolic composites and found that the mechanical and thermal properties of phenolic-polymer matrix composites were significantly improved by the addition of carbon materials as reinforcement. They also found that both carbon fiber and carbon nanotube/phenolic composites exhibited much better thermal conductivity and ablation properties than neat phenolic resins.[30] Natali et al. studied the ablative properties of two carbon nanofiller-based composites, CB, and multi-walled carbon nanotubes (MWNTs), and used them to produce highly loaded (50 wt. %) phenolic composites. They found that the MWNT-based composite exhibited a higher thermal diffusivity and an erosion rate that was maximum above the flame plume. In addition, the CB-based system showed a thin charred region, whereas the MWNT-based was characterized by a thick and wide pyrolyzed zone.[31] Also, novel polymer-based composites have being studied to be used as insulator materials.[32–35] Mesoporous silica particles are a new type of reinforcement obtained by sol–gel, which contain an ordered porosity similar to that of a honeycomb with empty worm-like canals. Its unique properties such as high surface area, high pore content with a narrow distribution (2–10 nm), and good chemical and thermal stability make them potentially suitable as reinforcements in thermal insulation materials.[36] In a previous work, we studied the ablation resistance of phenolic resin/mesoporous silica particles and obtained promising results.[37] However, the results cannot necessarily be extended to more complex systems, as when continuous fibers are added to the formulation (as in the case of the standard MX-4926 material used by NASA). Thus, the aim of this work was to obtain and to characterize modified phenolic resin/carbon fiber composite materials, which can be used as TPSs. Mesoporous silica particles and CB were added to phenolic resin to evaluate their effect on the performance of the materials. The materials obtained were studied in terms of ablation resistance by means of the oxyacetylene torch test and the burned samples were examined by Scanning electron microscopy (SEM). Other properties such as glass transition temperature and modulus were measured by dynamic mechanical analysis to elucidate the degradation mechanisms involved.

Experimental

Materials

Resol-type phenolic resin was prepared using a formaldehyde-to-phenol molar ratio equal to 1.3 under basic conditions. The synthesis procedure has been explained in detail in a previous work.[38]

Two different kinds of particles were added to the mentioned resin: CB (Cabot Argentina SAIC) and mesoporous silica particles in a proportion of 20 and 30 wt. %. The synthesis and characterization of mesoporous silica particles have been explained in detail in a previous work.[37] Bidirectional carbon

fibers (Hexcel, 282Carbono 3K) were used as reinforcement in all composites.

The composite materials were named as follows, according to the matrix: phenolic (Ph), phenolic + 20% carbon black (Ph20CB), phenolic+30% carbon black (Ph30CB), phenolic+20% silica particles (Ph20SI), phenolic+30% silica particles (Ph30SI).

Methods

Manufacture of composites. Composites were obtained by compression molding in a heated press. The first part of the procedure was focused on obtaining a good dispersion of the particles in the phenolic matrix. To this end, the exact amounts of resin and particles were weighed and mixed mechanically at 120 r/min and sonicated at 160 W during 30 min. The addition of a solvent (acetone) was necessary due to the large increase in resin viscosity associated with the addition of solid particles to the polymer. Once a homogeneous mixture was obtained, the fibers were impregnated with a metallic roller. The solvent removal was controlled by measuring the weight after putting the laminates in an oven at 60 °C. The laminates were in the oven until all the solvent was released. The fibers were stacked into the mold, and the mold was closed and placed in the heated press. The curing cycle was divided in two parts: first in a press at 80 °C for 3 h at 20 bar, and then in an oven for 3 h at 100 °C, 3 h at 120 °C, 3 h at 150 °C and 4 h at 190 °C.[37] Eighteen sheets were stacked in the same direction to obtain 4 mm-thick materials with 50% by volume of fibers.

Characterization and testing. Dynamic light scattering (DLS) was done in aqueous solution with a non-ionic surfactant (Triton X-100). The equipment was a Zetasizer Nano S90 with a 632.8 nm laser.

Transmission electron microscopy (TEM) images of the mesoporous silica particles were obtained in an FE-TEM JEM-2100F, JEOL. TEM images of the reinforced resin were obtained in a TEM JEOL 100 CX-II. Samples were ultramicrotomed at room temperature to obtain sections with a nominal thickness of 100 nm.

Density was measured by pycnometry, using the Archimedes′ principle at 20 °C, using cyclohexane (Cicarelli) as test fluid. At least three measurements were performed for each system.

Fiber volume content was calculated theoretically by equation (1), based on the sample thickness achieved, the number of sheets of fiber used, the fiber density and the surface density, as follows

$$\Theta = \frac{n * \xi}{t * \rho} \quad (1)$$

where

Θ: fiber volume content,
n: number of sheets of fiber in the composite,
ξ: fiber surface density (g/m^2),
t: plate thickness (m), and
ρ: fiber density (g/m^3).

Dynamic mechanical analysis was carried out in a Q800 TA Instruments equipment, in three-point bending mode. The frequency was set at 1 Hz, and the temperature ramp was from 30 to 450 °C at a heating rate of 5 °C/min.

The ablation properties of the materials were measured by the oxyacetylene torch test (ASTM E285), by means of an equipment constructed in our laboratory (Figure 1). Samples of $10 \times 10 \times 0.4\,cm^3$ were placed at 1.9 cm of the torch and the heat flux was 550 W/cm^2. The flame was controlled by changing the oxygen and acetylene proportion. The back-face temperature of the samples was measured with a K-type thermocouple. The heat flow was obtained calibrating the torch with the procedure established in the ASTM E457 standard (Standard Test method for measuring heat-transfer rate using a thermal capacitance (slug) calorimeter). Copper was used as slug material and the temperature vs time curve was measured (Figure 2).

The insulation index, taken as the relation between the time to increase the temperature from 250 to 900 °C and the thickness of the sample was calculated by equation (2)

$$Insulation\ index = \frac{(t_{900^\circ C} - t_{250^\circ C})}{thickness} \quad (2)$$

where

$t_{900\,^\circ C}$: time in which the sample reach 900 °C (s)
$t_{250\,^\circ C}$: time in which the sample reach 250 °C (s)
thickness: thickness of the sample (m)

SEM images were obtained in a JEOL JSM-6460LV microscope. For this, the samples were dried and coated with a thin layer of gold (300 Å).

Results and discussion

Characterization of fillers

Different textural and structural characterization tests were performed in both fillers, CB and silica particles, before its mixing with the phenolic matrix. DLS tests were performed in CB particles in order to obtain the size distribution, while SEM and TEM were used to characterize the size and structure of mesoporous silica particles.

Figure 1. Oxyacetylene torch test equipment scheme.

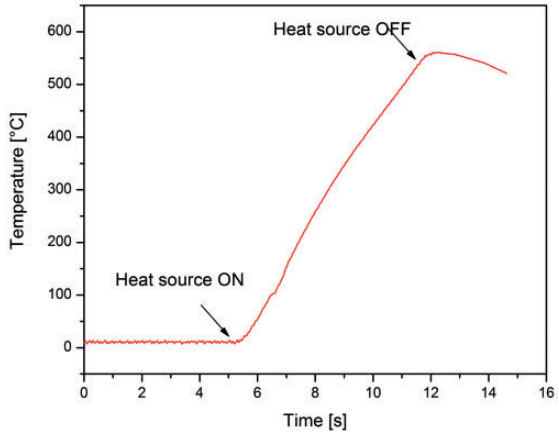

Figure 2. Temperature as a function of time measured during the calibration of the torch test equipment.

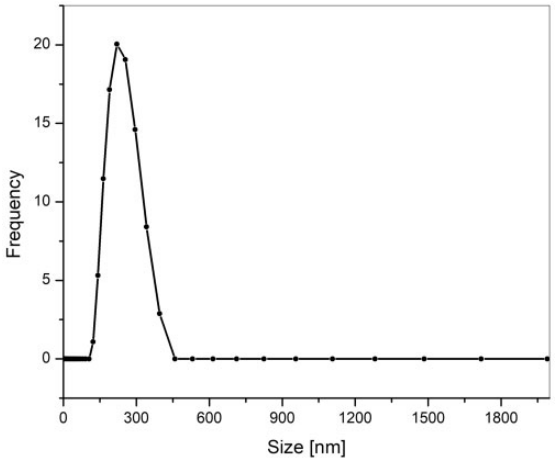

Figure 3. DLS curve obtained for the CB filler in aqueous solution.

Regarding the size distribution, it is not common to refer to the particle diameter when the material to be treated is CB. That is, during the characterization it is appropriate to refer directly to the agglomerates that are formed by the coalescence of ultra fine particles. The DLS curve for the CB particles is presented in Figure 3, it can be seen that the average size of the agglomerates is 300 nm and that the distribution is narrow.

Regarding the silica particles, the images obtained by SEM and TEM are presented in Figure 4(a) and (b), respectively. In the Figure 4(a), it can be seen agglomerates with a size distribution of the order of microns, and the or worm-like morphology characteristic of this type of particles, results are in agreement with those reported in the literature.[39] The structure of mesopores was visualized through TEM (Figure 4(b)). The obtained images demonstrate the presence of a regular pore structure in the particles; the uniform channels correspond to what is reported in the literature.[40]

CB and silica particles X-ray patterns are presented in a previous work,[37] results are in accordance with those presented in bibliography.

Also, before the composites processing, the dispersion of the particles in the phenolic matrix was studied by TEM. Only the images of the composites with 20 wt. % of filler were analyzed for both types of reinforcements. It can be seen in the photographs in Figure 5(a) and (b) that a good dispersion was obtained for both materials. In the materials with silica particles, mesoporosity is clearly seen, and darker areas are associated to overlapping of two or more particles. In the materials with CB the spherical aggregates can be observed,

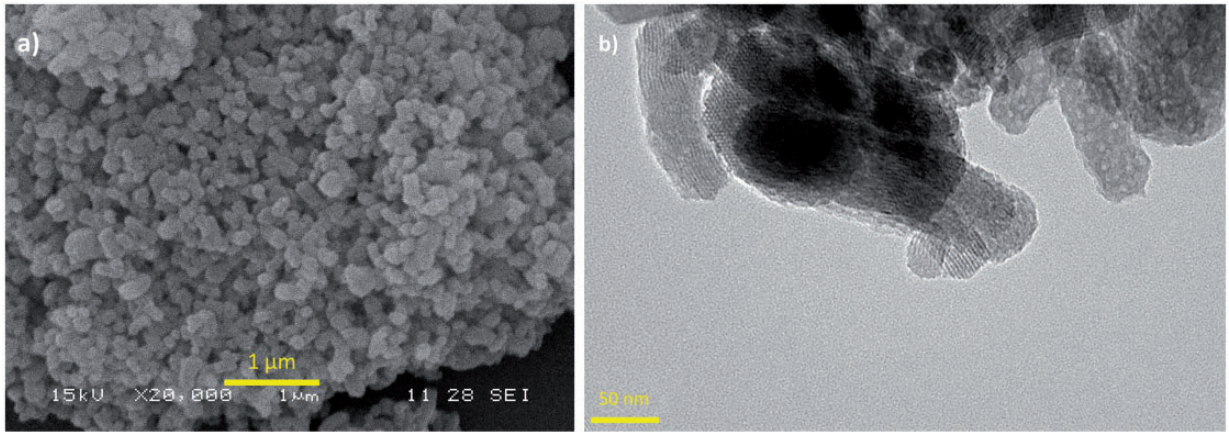

Figure 4. (a) SEM and (b) TEM of the mesoporous silica particles used as filler in the phenolic resin.

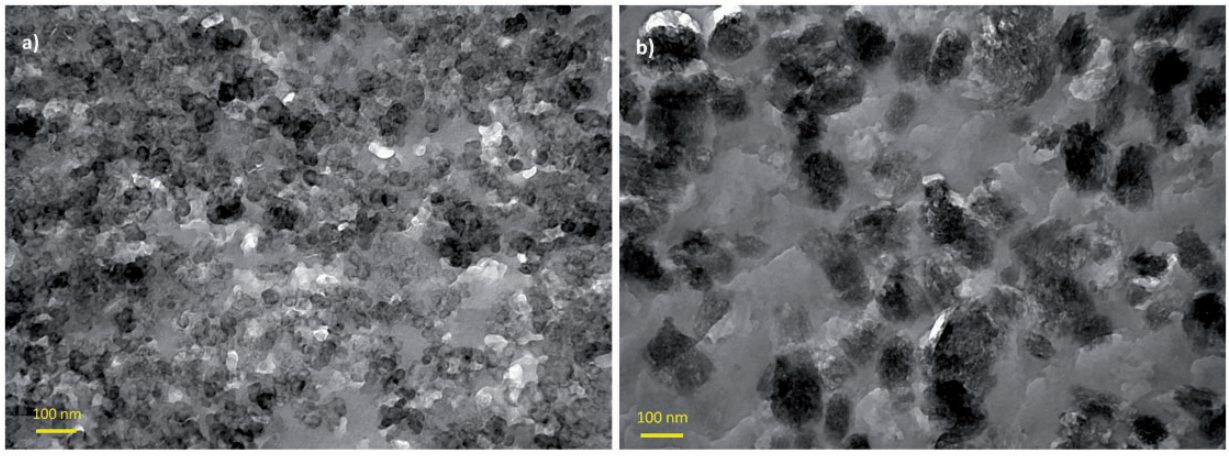

Figure 5. TEM images of (a) phenolic resin with 20 wt.% of CB (b) phenolic resin with 20 wt.% of mesoporous silica particles.

each aggregate is made up of elementary particles of about 50 nm. A good dispersion in the phenolic resin was confirmed.

Composites

When composites are used as ablatives for thermal protection, density must be taken into account. A decrease in the total weight of space rockets by using materials with better properties will result in a reduction in the amount of fuel used or an increase in the payload.

The density values in the present study (Table 1) are in agreement with others reported for similar composites.[41,42] When comparing the density values, it can be seen that adding particle loads to the composites induced an increase in density, which would be counterproductive for the application proposed. This result was expected because the loads added were denser than the polymer matrices, whose density is always close to 1.1 g/cm^3.

Table 1. Composite materials' density.

Material	Density (g/cm^3)
Ph11	1.26 ± 0.01
Ph14	1.22 ± 0.02
Ph18	1.30 ± 0.04
Ph20CB	1.45 ± 0.03
Ph30CB	1.46 ± 0.05
Ph20SI	1.38 ± 0.01
Ph30SI	1.41 ± 0.01

Dynamic mechanical tests were conducted to evaluate the effect of particle incorporation on the microstructure of the polymer network. The variation in the glass transition temperature (Tg) and the storage

Table 2. Modulus and glass transition temperature obtained by Dynamic mechanical analysis (DMA) for composites.

Material	Modulus (GPa)	Tg (°C)
Ph	42.7 ± 2.1	376
Ph20CB	27.1 ± 0.9	302
Ph30CB	–	–
Ph20SI	28.5 ± 1.2	299
Ph30SI	12.5 ± 0.6	295

modulus (E') of the materials was recorded as a function of the particle concentration (results are presented in Table 2). Tg was measured as the temperature that corresponds with the maximum of the tanδ peak, whereas E' in the glassy state was measured at 35 °C. In a previous work,[43] we observed a reduction in the crosslinking density with the incorporation of both types of particles. This is because particles act as discontinuous points for the polymer network, decreasing the crosslinking capacity. However, in the case of silica particles, the reduction was slighter, which was attributed to the chemical interaction between the hydroxyl groups of the phenolic resin and the silanols of the silica particles. These structural changes when particles were incorporated explain the decrease in both Tg and E' for silica- and CB-modified composites.

To evaluate the ablation resistance of the materials, it was necessary to simulate the aggressive conditions of the hyper-thermal environment at which TPSs are subjected (high heat fluxes and very high temperatures). The oxyacetylene torch test (ASTM E285) is the most frequently applied and cost-effective way to measure the ablative resistance of materials at a laboratory scale. The test consists in exposing a sample to the flame and recording the time it takes to be passed through. This time is then used to calculate the erosion rate.

The first part of the analysis was centered in the study of the effect of fiber content on the ablation resistance of the composites in the torch test. To this end, we studied samples based on phenolic resin and carbon fibers with different fiber volume contents. Composites with 11, 14, and 18 sheets of fiber (keeping constant the thickness of the samples) were processed by compression molding and tested. The erosion rate of the composites was compared with the erosion rate of the neat resin tested in the same conditions.[37] Results are presented in Figure 6. The erosion rate was lowest in the system with 18 layers of fiber (largest fiber volume percent), and increased as the fiber content increased. This highlights the incidence of the carbon fiber content in the response of the materials against fire. Besides providing mechanical strength and stability

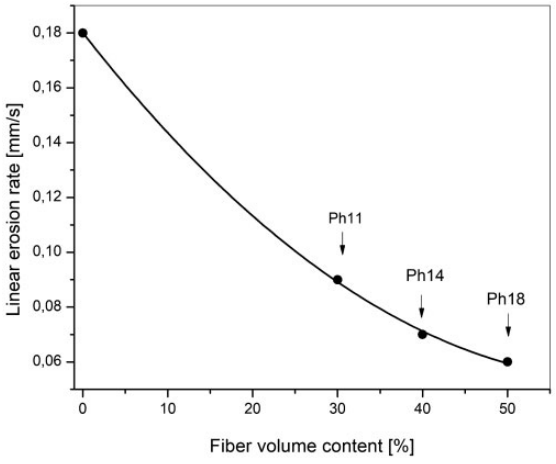

Figure 6. Effect of fiber content on the erosion rate of phenolic resin/carbon fiber composites.

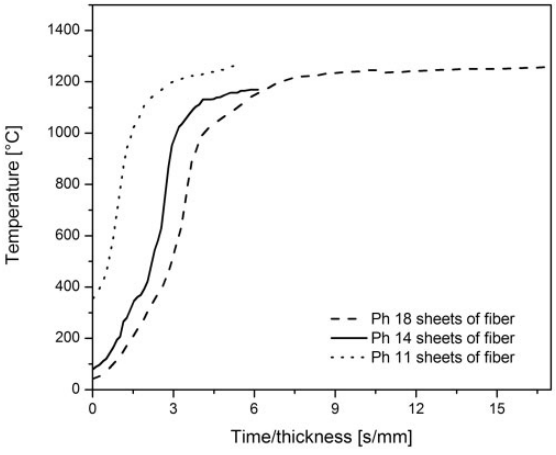

Figure 7. Temperature vs time/thickness for the composites of phenolic resin with 11, 14, and 18 sheets of carbon fiber.

to the *char*, carbon fibers absorb energy and re-radiate it, making the material more resistant to the flame.

When we analyzed the temperature rise during the test (Figure 7), we observed that the material with 18 layers of fiber had better insulation properties, i.e. the time required to achieve certain temperature increased as the fiber volume content increased. Then, the phenolic matrix of the composites was modified through the addition of different types and percentages of nanoparticles and the influence of the nanoparticles on the ablative behavior of the composites was studied by the torch test. The fiber volume contents of the composites are listed in Table 3. Several parameters derived from the torch test performed on the composites, including the linear erosion rate, the mass erosion rate (calculated with the mass variation during the torch test and the burn-through-time) and the insulation index (taken as the relation between the time to increase the

Table 3. Ablation properties of phenolic resin/carbon fiber composites.

Material	Fiber volume content (%)	Linear erosion rate (mm/s)	Mass erosion rate (g/s)	Insulation index (s/m)
Ph	49.2 ± 0.7	0.060 ± 0.004	0.149 ± 0.008	1693 ± 102
Ph20CB	43.3 ± 1.0	0.063 ± 0.007	0.150 ± 0.005	1916 ± 123
Ph30CB	44.6 ± 0.7	0.058 ± 0.009	0.140 ± 0.024	3321 ± 109
Ph20SI	45.0 ± 1.0	0.064 ± 0.004	0.129 ± 0.007	2780 ± 136
Ph30SI	39.9 ± 1.0	0.065 ± 0.005	0.136 ± 0.012	2570 ± 119

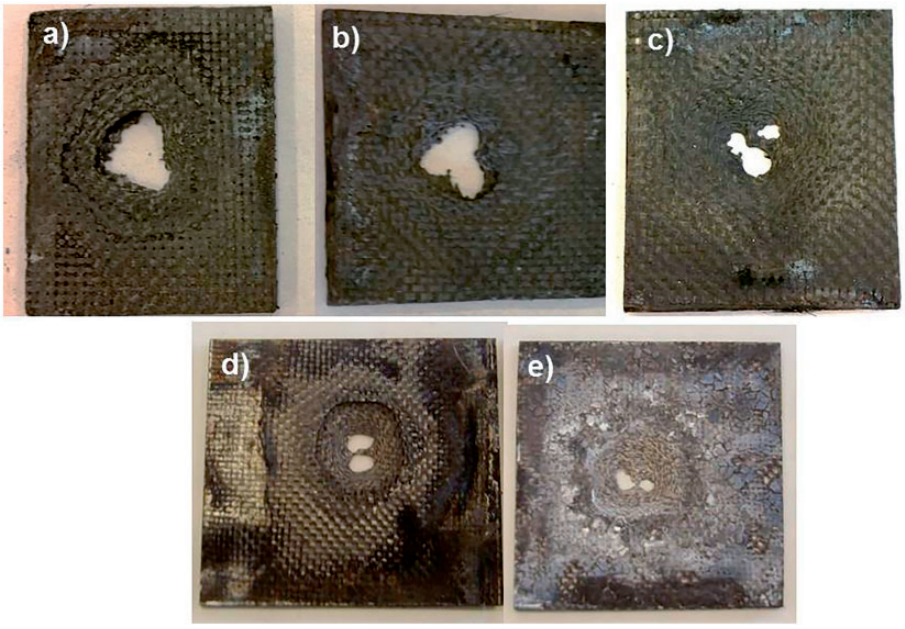

Figure 8. Plates after torch test. (a) Ph 11 sheets of fiber, (b) Ph 14 sheets of fiber, (c) Ph 18 sheets of fiber, (d) Ph20CB, and (e) Ph20SI.

temperature from 250 to 900 °C and the thickness of the sample, equation (2)), are also reported in Table 3.

A first aspect to consider was that, although we processed all the samples with 18 layers of fiber (except for the plates that were obtained to evaluate the effect of varying the fiber content), the fiber volume fraction varied between the different systems. Less than 50% of fiber volume content was obtained in all the samples with particulate fillers in the matrix. This was attributed to the increase in the viscosity of the resin and the compaction resistance caused by the incorporation of solid fillers in the composite. This difference was taken into account when comparing the erosion rate values.

The results shown in Table 3 allow determining that the systems with lowest linear erosion rate were those containing CB and silica particles, with differences between them that were within the range of error.

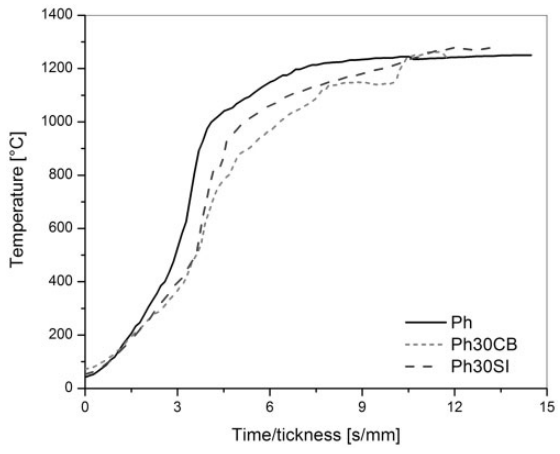

Figure 9. Temperature vs time/thickness for composites with carbon black and silica particles.

The material with phenolic resin without nanoparticles had a low linear erosion rate. However, when analyzing the fiber content and considering an interpolation of the results (Figure 6), we observed that for fiber contents similar to those obtained in CB and silica particulate formulations (about 45%), the erosion rate would be clearly higher.

In the case of the material with CB, the behavior was justified by the ability of this filler to promote the formation of *char*,[31] which delays the degradation of the composite, reducing the erosion rate. In contrast, in the case of the material with mesoporous silica particles, the behavior was attributed to its lower thermal conductivity, given by the internal porosity of the particles, and its permanence on the fibers after the complete degradation of the resin.

The tendency observed in the behavior of the materials against the flame was the same as that observed in our previous work,[37] although the effect of the nanoparticles was not as strong, due to the mask effect of the high fiber content of the composites.

When analyzing the mass erosion rate, which represents the structural loss of material during the test, a decrease of this value was observed in the materials

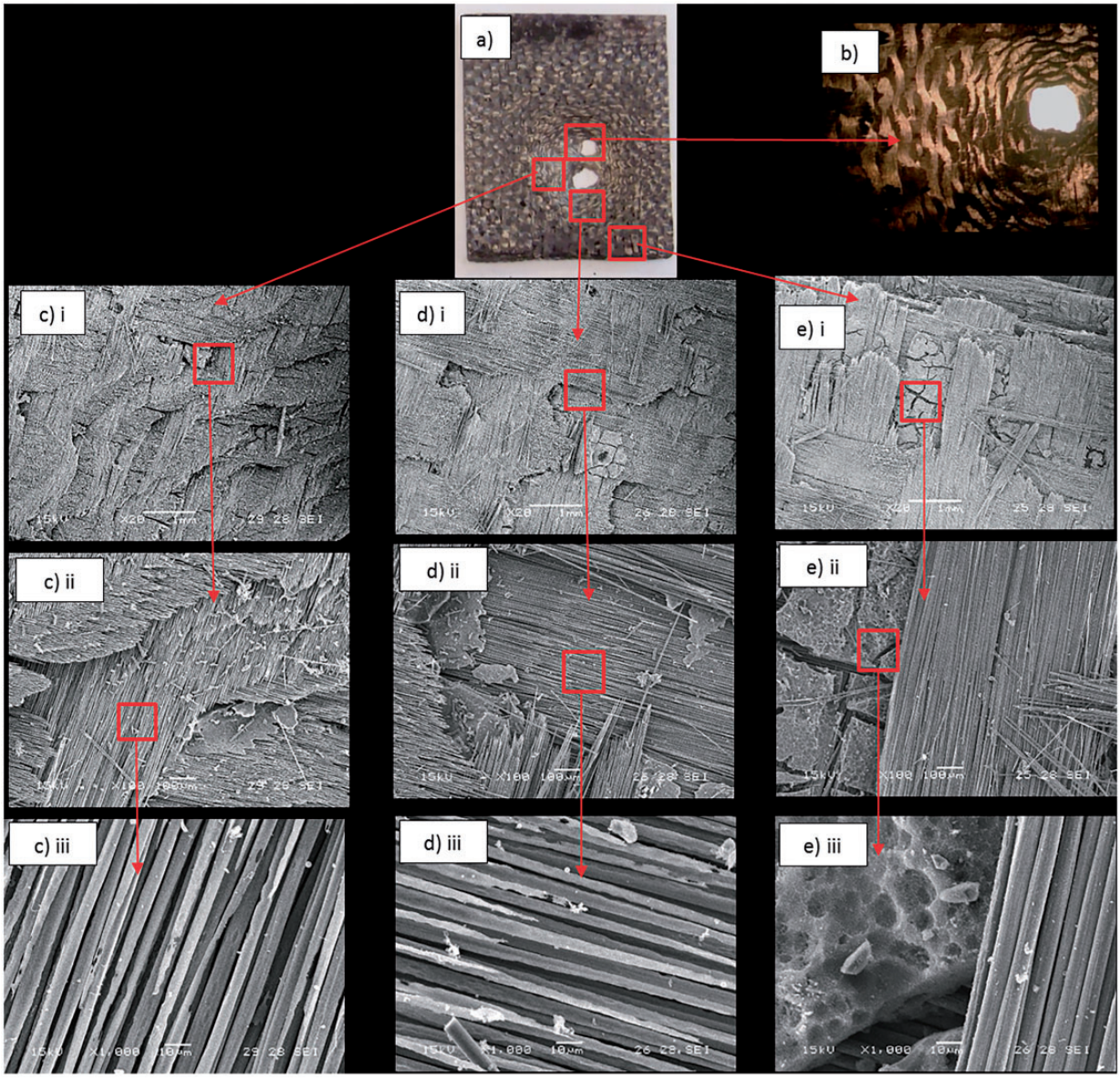

Figure 10. Composite material with 20 wt. % of CB (a) plate post torch test, (b) microscope image 3.5×. SEM images: (c) area closest to the flame, (d) medium area, (e) area away from flame; (i) 20×, (ii) 100×, (iii) 1000×.

with mesoporous silica particles. This may be associated with a greater integrity of the *char* layer in the area surrounding the point of contact with the flame and with a more localized damage. These results are of great importance since they represent the stabilization of the carbonaceous residue by the addition of the silica particles on the matrix, and it can be inferred that, in an application where the exposure to the flame is less localized, the material could present a better behavior than that of standard materials.

It should be considered that, during the oxyacetylene test, the flame impacts the composite material perpendicularly, giving the most aggressive condition. In spacecraft nozzles, the fibers are located in a configuration that makes the flames and the erosive particles that are ejected at high velocities to impact the composite practically parallel to the surface.[44]

Some images of the plates after the torch tests are presented in Figure 8 and are consistent with images of composite materials of similar formulations.[30] Samples with lower fiber content showed a more widespread damage, which is consistent with the lower ablation resistance obtained in the test. As the fiber content increase, the size of the hole is reduced. Samples with

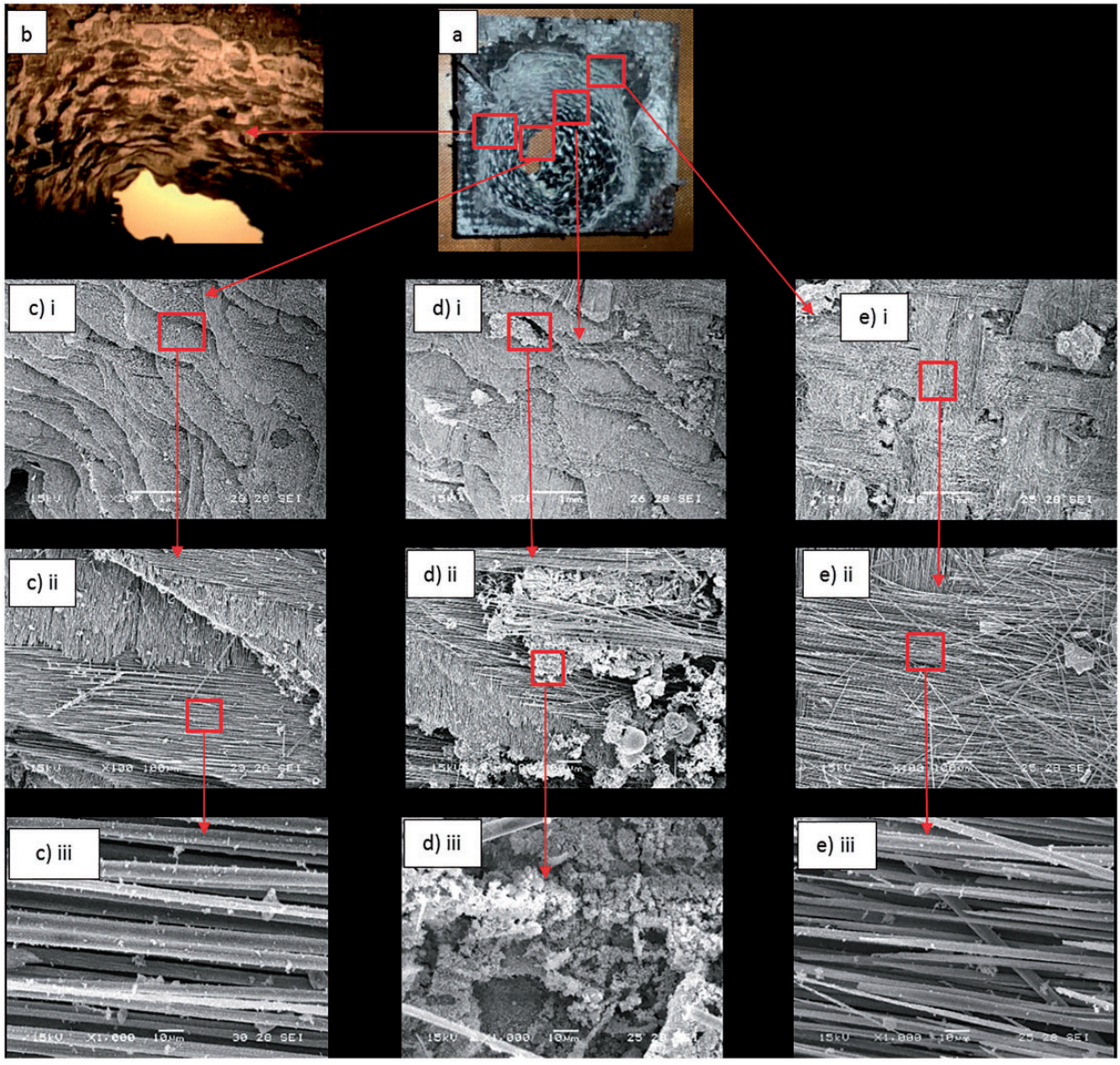

Figure 11. Composite material with 20 wt. % of silica particles (a) plate post torch test, (b) microscope image 3.5×. SEM images: (c) area closest to the flame, (d) medium area, (e) area away from flame; (i) 20×, (ii) 100×, (iii) 1000×.

CB and silica particles showed a more localized damage, which is a consequence of the stabilization of the char produced by the fillers.

The insulation index reported in Table 3 was analyzed together with the results shown in Figure 9. This analysis showed that the lowest index corresponds to the phenolic system, which means that the addition of micro- and nano-reinforcements generates an increase in isolation capacity of the composite with phenolic resin. The highest insulation capacity was achieved by the composite with 30 wt. % of CB. Although insulation indices characterize the insulation behavior at low temperatures, the results are affected by local phenomena of the test and do not always represent an intrinsic property of the material. For example, a material in which the fiber sheets are separated by the action of the flame will have very little ablation resistance, but the insulation index may be high, since separate (but not yet detached) layers may act as a heat shield during the first few seconds of the test.

After being tested, the burnt plates were examined using optical microscopy and SEM to identify differences in the carbon residue generated by the composites. The images obtained for the composite with a phenolic resin matrix with 20 wt. % CB and 20 wt. % of mesoporous silica particles are shown respectively in Figures 10 and 11.

It is generally observed that the damage occurred by layers. That is once the resin pyrolyzes and is consumed by the ablative process, the carbon fibers begin to be damaged, and because of the erosion generated during the process, fiber layers are also degraded, giving rise to new surfaces that will then be consumed by the same process. In turn, as the material is removed, oxygen is allowed to enter more easily and the oxidation and degradation process is accelerated.[5,29,41] This behavior, as well as zones with damaged and cut fibers,[45] can be clearly observed in the images with less magnification (Figures 10(b) to 11(b)).

The material with mesoporous silica particles presented a white residue generated by the silica content of the matrix, whose appearance is similar to that reported in phenolic resin-based composites with inorganic fillers and carbon fibers.[41]

When comparing the images with greater magnification, in the area nearest to the flame, we found that, in the composite material with CB, the fibers were almost ''clean'', i.e. without remains of resin or CB particles. Instead, in the case of composites with mesoporous silica particles, remains of particles were found on the surface of the fibers.[41] This would indicate that the torch has not removed the melt silica, which may contribute to increasing the ablation resistance of this material.

Conclusions

In this work, we studied the influence of the addition of CB and mesoporous silica particles on the ablative properties of phenolic/carbon fiber-based composites. The introduction of CB and silica particles in the phenolic matrix decreased its glass transition temperature and the composite flexural modulus. However, regarding the ablation properties, the composite with 30 wt. % of CB showed the lowest linear erosion rate (0.058 mm/s) and the highest insulation index, denoting the ability of the *char* produced to protect the virgin material. Considering that such composite has 44% by volume of carbon fibers, it could be inferred that its properties could be improved by increasing the fiber content and maintaining the amount of CB.

The composite with 20 wt. % of mesoporous silica particles exhibited the lowest mass erosion rate (0.129 g/s), indicating that the damage was more localized and that the melt silica (observed as white areas in the burnt plates) remained above the carbon fibers, protecting the surface of the material during fire exposure.

Hence, this new kind of carbon/phenolic composite has great potential for applications in thermal insulation and TPSs for the aerospace industry.

Declaration of Conflicting Interests

The author(s) declared no potential conflicts of interest with respect to the research, authorship, and/or publication of this article.

Funding

The author(s) disclosed receipt of the following financial support for the research, authorship, and/or publication of this article: The authors would like to thank to the National Council of Scientific and Technical Research (CONICET), The National University of Mar del Plata and National Agency of Scientific and Technological Promotion, ANPCyT (grant code PICT 2013 2455).

ORCID iD

ES Rodríguez http://orcid.org/0000-0001-7617-868X

References

1. Bahramian AR and Kokabi M. Polymer nanocomposites as ablative materials. In: *Polymer Green Flame Retardant*. Amsterdam: Elsevier, 2014, pp.461–502.
2. Bahramian AR, Kokabi M, Famili MNH, et al. Ablation and thermal degradation behavior of a composite based on resol type phenolic resin: process modeling and experimental. *Polymer* 2006; 47: 3661–3673.
3. Cho D, Lee JY and Yoon BI. Microscopic observations of the ablation behaviours of carbon fibre/phenolic composites. *J Mater Sci Lett* 1993; 12: 1894–1896.

4. Natali M, Kenny JM and Torre L. Science and technology of polymeric ablative materials for thermal protection systems and propulsion devices: a review. *Prog Mater Sci* 2016; 84: 192–275.
5. Chen Y, Chen P, Hong C, et al. Improved ablation resistance of carbon–phenolic composites by introducing zirconium diboride particles. *Compos Part B* 2013; 47: 320–325.
6. Choi MH, Byun HY and Chung IJ. The effect of chain length of flexible diacid on morphology and mechanical property of modified phenolic resin. *Polymer* 2002; 43: 4437–4444.
7. Pilato L. Phenolic resins: 100 years and still going strong. *React Funct Polym* 2012; 73: 270–277.
8. Eslami Z, Yazdani F and Mirzapour MA. Thermal and mechanical properties of phenolic-based composites reinforced by carbon fibres and multiwall carbon nanotubes. *Compos Part A* 2015; 72: 22–31.
9. Schmidt DL and Craig RD. *AFWAL US, AFWAL-TR-81-4136*, 1982.
10. Minges ML. Thermophysical characteristics of high-performance ablative composites. In: D'Aelio GF and Parker JA (eds) *Ablative plastics*. New York: Marcel Dekker Inc., 1971, pp.287–312.
11. Koo JH. *Polymer nanocomposites: processing, characterization, and applications*. New York: McGraw-Hill Professional, 2006, pp.159–76.
12. Cortopassi AC. *Erosion of carbon-cloth phenolic nozzles in rocket motors with aluminized solid propellant A Ph.D. dissertation in Mechanical Engineering*. The Pennsylvania State University, The Graduate School, College of Engineering, 2012.
13. Cortopassi AC, Boyer E and Kuo KK. Update: a subscale solid rocket motor for characterization of submerged nozzle erosion. In: *45th AIAA/ASME/SAE/ASEE joint propulsion conference & exhibit*, 2–5 August 2009, Denver, Colorado.
14. *Cyted MX-4926 datasheet*, 2015. https://www.e-aircraftsupply.com/MSDS/81124cytec%20MX-4926N%20tds.pdf
15. Vaia RA, Price G, Ruth PN, et al. Polymer/layered silicate nanocomposites as high performance ablative materials. *Appl Clay Sci* 1999; 15: 67–92.
16. Natali M and Torre L. Ablative materials. In: *Wiley encyclopedia of composites*. New York: Wiley, 2011, pp.1–14.
17. Bahramian AR and Kokabi M. Ablation mechanism of polymer layered silicate nanocomposite heat shield. *J Hazard Mater* 2009; 166: 445–454.
18. Ghelich R, Aghdam RM and Jahannama MR. Elevated temperature resistance of SiC-carbon/phenolic nanocomposites reinforced with zirconium diboride nanofibers. *J Compos Mater* 2017; DOI: 10.1177/0021998317723447.
19. Shi S, Gong C, Liang J, et al. Ablation mechanism and properties of silica fiber-reinforced composite upon oxy-acetylene torch exposure. *J Compos Mater* 2016; 50: 3853–3862.
20. Shi S, Liang J, Yi F, et al. Modeling of one-dimensional thermal response of silica-phenolic composites with volume ablation. *J Compos Mater* 2012; 47: 2219–2235.
21. Wang S, Wang Y, Bian C, et al. The thermal stability and pyrolysis mechanism of boron-containing phenolic resins: the effect of phenyl borates on the char formation. *Appl Surf Sci* 2015; 331: 519–529.
22. Robert TM, Chandran MS, Jishnu S, et al. Nanoclay modified silica phenolic composites: mechanical properties and thermal response under simulated atmospheric re-entry conditions. *Polym Adv Technol* 2015; 26: 104–109.
23. Yum SH, Kim SH, Lee WI, et al. Improvement of ablation resistance of phenolic composites reinforced with low concentrations of carbon nanotubes. *Compos Sci Technol* 2015; 121: 16–24.
24. Li C, Ma Z, Zhang X, et al. Silicone-modified phenolic resin: relationships between molecular structure and curing behavior. *Thermochim Acta* 2016; 639: 53–65.
25. Liu C, Li K, Li H, et al. The effect of zirconium incorporation on the thermal stability and carbonized product of phenol-formaldehyde resin. *Polym Degrad Stabil* 2014; 102: 180–185.
26. Srikanth I, Padmavathi N, Kumar S, et al. Mechanical, thermal and ablative properties of zirconia, CNT modified carbon/ phenolic composites. *Compos Sci Technol* 2013; 80: 1–7.
27. Zhang Y, Shen S and Liu Y. The effect of titanium incorporation on the thermal stability of phenol-formaldehyde resin and its carbonization microstructure. *Polym Degrad Stabil* 2013; 98: 514–518.
28. Srikanth I, Daniel A, Kumar S, et al. Nano silica modified carbon–phenolic composites for enhanced ablation resistance. *Materialia* 2010; 63: 200–203.
29. Ding J, Huang Z, Qin Y, et al. Improved ablation resistance of carbon/phenolic composites by introducing zirconium silicide particles. *Compos Part B* 2015; 82: 100–107.
30. Park JM, Kwon DJ, Wang ZJ, et al. Effects of carbon nanotubes and carbon fiber reinforcements on thermal conductivity and ablation properties of carbon/phenolic composites. *Compos Part B* 2014; 67: 22–29.
31. Natali M, Monti M, Puglia D, et al. Ablative properties of carbon black and MWNT/phenolic composites: a comparative study. *Compos Part A* 2012; 43: 174–182.
32. Ogasawara T, Ishikawa T and Yamada T. Thermal response and ablation characteristics of carbon fiber reinforced composite with novel silicon containing polymer MSP. *J Compos Mater* 2002; 36: 143–157.
33. Parkar Z, Mangun C, King D, et al. Ablation characteristics of an aromatic thermosetting copolyester/carbon fiber composite. *J Compos Mater* 2011; 46: 1819–1830.
34. Ahmed AF and Hoa SV. Thermal insulation by heat resistant polymers for solid rocket motor insulation. *J Compos Mater* 2011; 46: 1549–1559.
35. Cheng H, Xue H, Hong C, et al. Preparation, mechanical, thermal and ablative properties of lightweight needled carbon fibre felt/phenolic resin aerogel composite with a bird's nest structure. *Compos Sci Technol* 2017; 140: 63–72.
36. Cooper C and Burch R. Mesoporous materials for water treatment processes. *Water Res* 1999; 33: 3689–3694.
37. Asaro L, Manfredi LB, Pellice S, et al. Innovative ablative fire resistant composites based on phenolic resins

modified with mesoporous silica particles. *Polym Degrad Stab* 2017; 177: 7–16.
38. Asaro L, Rivero G, Manfredi LB, et al. Development of carbon fiber/phenolic resin prepregs modified with nanoclays. *J Compos Mater* 2016; 50: 1287–1300.
39. Bippus L, Jaber M, Lebeau B, et al. Thermal conductivity of heat treated mesoporous silica particles. *Microporous Mesoporous Mater* 2014; 190: 109–116.
40. Xie M, Shi H, Ma K, et al. Hybrid nanoparticles for drug delivery and bioimaging: mesoporous silica nanoparticles functionalized with carboxyl groups and a near-infrared fluorescent dye. *J Colloid Interface* 2013; 395: 306–314.
41. Mirzapour A, Asadollahi MH, Baghshaei S, et al. Effect of nanosilica on the microstructure, thermal properties and bending strength of nanosilica modified carbon fiber/phenolic nanocomposites. *Compos Part A* 2014; 63: 159–167.
42. Bian L, Xiao J, Zeng J, et al. Microstructural interpretation of the ablative properties of phenolic–quartz hybrid fabric reinforced phenolic resin composites. *Mater Des* 2014; 62: 424–429.
43. Asaro L, D'Amico DA, Alvarez VA, et al. Impact of different nanoparticles on the thermal degradation kinetics of phenolic resin nanocomposites. *J Therm Anal Calorim* 2017; 128: 1463–1478.
44. Lawrence T, Beshears R, Burlingame S, et al. Fabrication of composite combustion chamber/nozzle for fastrac engine. In: *4th conference on aerospace materials, processes, and environmental technology; (NASA/CP-2001-210427)*, NASA Marshall Space Flight Center; Huntsville, AL US, 3 August 2001.
45. Cho D and Yoon BI. Microstructural interpretation of the effect of various matrices on the ablation properties of carbon-fiber-reinforced composites. *Compos Sci Technol* 2001; 61: 271–280.